# Modeling the coverage of an AFM tip by enzymes and its application in nanobiosensors

Adriano M. Amarante [a], Guedmiller S. Oliveira [a,*], Carolina C. Bueno [a], Richard A. Cunha [b], Jéssica C.M. Ierich [a], Luiz C.G. Freitas [c], Eduardo F. Franca [b], Osvaldo N. Oliveira Jr. [d], Fábio L. Leite [a,*]

[a] Nanoneurobiophysics Research Group, Department of Physics, Chemistry and Mathematics, Federal University of São Carlos, 18052-780 Sorocaba, SP, Brazil
[b] Chemistry Institute, Federal University of Uberlândia, 38400-902 Uberlândia, MG, Brazil
[c] Chemistry Department, Federal University of São Carlos, 13565-905 São Carlos, SP, Brazil
[d] São Carlos Institute of Physics, University of São Paulo, 13566-590 São Carlos, SP, Brazil

## A B S T R A C T

A stochastic simulation of adsorption processes was developed to simulate the coverage of an atomic force microscope (AFM) tip with enzymes represented as rigid polyhedrons. From geometric considerations of the enzyme structure and AFM tip, we could estimate the average number of active sites available to interact with substrate molecules in the bulk. The procedure was exploited to determine the interaction force between acetyl-CoA carboxylase enzyme (ACC enzyme) and its substrate diclofop, for which steered molecular dynamics (SMD) was used. The theoretical force of $(1.6 \pm 0.5)$ nN per enzyme led to a total force in remarkable agreement with the experimentally measured force with AFM, thus demonstrating the usefulness of the procedure proposed here to assist in the interpretation of nanobiosensors experiments.

© 2014 Elsevier Inc. All rights reserved.

## 1. Introduction

Nanobiosensors are highly sensitive and selective sensors with nanoscale resolution (1–100 nm) [1], which can be based on atomic force microscopy (AFM). Since with AFM one is capable of measuring forces of the order of magnitude of a chemical bond [2], specific molecular detection can be achieved in the so-called Chemical Force Microscopy (CFM). Various combinations of sensing molecules (e.g. enzymes, antibody) and substrates (e.g. inhibitors, antigens) can be used to build nanobiosensors with AFM. The design of an effective sensor, however, requires understanding of the specific interactions leading to detection signals, such as those generated by enzyme-inhibitor pairs [3–6]. Owing to the complexity of the enzyme–substrate interaction, in silico studies are now employed, including molecular dynamics (MD) simulations [7–9]. With the present computational capabilities, even using enhanced sampling techniques, the simulation of these interactions cannot be made at the atomistic level due to the size of the system and the time scale of the phenomena taking place during operation of a nanobiosensor [10–12]. Therefore, the development of approximated methodologies is needed.

In this study, a coarse grained model is proposed to determine the interaction between acetyl-CoA carboxylase (ACC) and diclofop, a commercial herbicide known to block ACC activity by occupying its binding pocket [13–17] in a non-covalent, reversible interaction. The coarse-grained model for the AFM tip surface covered by enzymes uses atomistic information obtained from MD simulations and technical specifications from the manufacturer of the AFM tip. The model was used to determine the average interaction energy per active site while the number of active sites available to interact with the herbicide substrate was obtained using a stochastic model, where the enzymes were represented by polyhedrons adsorbing on the tip. The theoretical forces are compared to experimentally obtained values.
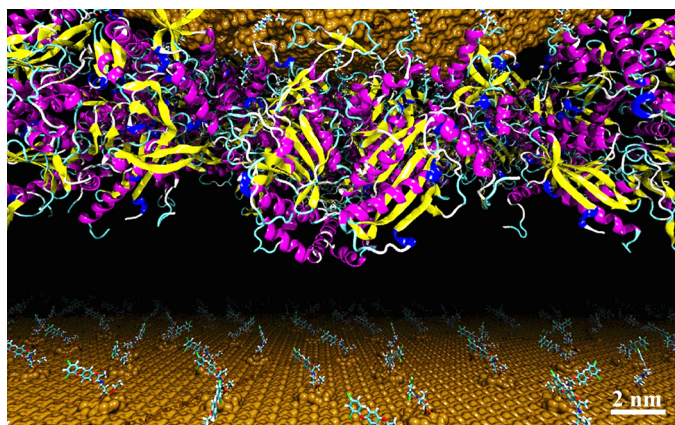
## 2. Methodology

### 2.1. ACC as dimeric structure

The initial structure of the ACC enzyme, shown in Fig. 1, was obtained from the Protein Data Bank online repository [18] under

* Corresponding authors. Tel.: +55 15 3229 6014.
*E-mail addresses:* guedmuller@gmail.com (G.S. Oliveira), fabioleite@ufscar.br (F.L. Leite).

**Fig. 1.** Artwork of the ACC enzymes arrangement on the AFM tip and substrate surface with functionalized diclofop molecules for detection.

**Table 1**
Number of actives sites available according to the polyhedron faces orientations.

| Faces | Contact area (nm$^2$) | Covered area of the AFM tip (nm$^2$) | Active sites available |
|---|---|---|---|
| 1 | 42.4 | 33.9 | 0 |
| 2 | 42.4 | 33.9 | 0 |
| 3 | 30.2 | 36.7 | 1 |
| 4 | 30.2 | 36.7 | 1 |
| 5 | 17.0 | 33.9 | 1 |
| 6 | 17.0 | 33.9 | 1 |

PDB ID 1UYR. The enzyme was assumed to adopt a dimeric conformation in solution, according to molecular dynamics simulation with an all-atom model [19,20]. The coverage of the AFM tip with the enzymes was simulated with a stochastic process in MD simulations, where a coarse-grained model had to be used. The enzyme dimers were represented as rigid structures, as already applied in molecular docking calculations of inhibitor-enzyme interactions [21,22]. The use of a rigid model is justified based on the stability of the dimeric structures. Indeed, a stable dimeric ACC structure was reached within 10 ns of MD trajectory with a RMSD of 0.3 nm [19], whereas the dimeric structure was attached to a functionalized surface, it remained stable within a RMSD of 0.35 nm after a 50 ns MD trajectory [20].

### 2.2. Stochastic coverage of the AFM tip

The dimeric form of ACC was represented by a polyhedron with six faces, which dimensions A through F, depicted in Fig. 2, were obtained using the procedures described in [23,24] with the MD data by Franca et al. [19]. Because the charge distribution on the ACC enzyme dimer surface is homogeneous [19], there is no preferential region for enzyme adsorption on the AFM tip. Therefore, the enzyme-surface energy interaction will be assumed proportional to the contact area, and so will be the probability of each of the six faces (A–F) of the polyhedron to be in contact with the AFM tip. The adsorption process is then assumed to be stochastic with adsorption probability proportional to the contact area, which is defined in Fig. 2. As a consequence of the ACC dimer symmetry a twofold degeneracy is found between faces {A, B}, {C, D} and {E,F}. Hence, there are only three energetically distinct attachment positions.

### 2.3. Number of functionalized enzymes on the AFM tip surface

For a given configuration of polyhedrons covering the tip surface, geometric considerations can be used to determine the availability of the enzyme cavity to interact with substrates from the bulk. The number of ACC dimers attached to the AFM tip, which are effective for interacting with substrates, is required to normalize the signal measured in an AFM experiment. This number depends on geometrical parameters of the substrates as well as on the density of enzyme dimers on the AFM tip surface. The latter density depends on the tip radius and on the average area occupied by a single enzyme dimer. Fig. 3 shows a monolayer of adsorbed enzyme dimers which will effectively interact with the substrate molecules from the bulk.

The ACC dimer hydration energy calculated by Franca et al. [19] is $-23.36 \cdot 10^3$ kJ/mol, and its isoelectric point is 6.23 [25]. As the hydration energy is small and electrostatic repulsion can be neglected, we assume that the AFM tip surface is uniformly covered by ACC dimers represented by rigid polyhedrons. The spherical AFM tip area $A$ is calculated using $A = 2\pi\delta R$, where $R$ is the radius given by the manufacturer [26] and $\delta$ is a parameter depending on the substrate geometry as indicated in Fig. 3. The calculated area for the AFM tip available for adsorption is $A = (220 \pm 31)$ nm$^2$.

A modeling software [23,24] was employed to obtain distributions of polyhedron conformations that could be adsorbed on the tip surface. The contact area for each face, and the area of the AFM tip covered by a given face were determined in Table 1. Also included in the table, the availability of the active site is showed. The stochastic program [27] to obtain sets of configurations for the adsorption of polyhedrons has a 4-step procedure, as follows:

Step 1: choose the number $N$ of dimers on the surface.
Step 2: sort a given polyhedron face. For a given polyhedron face its Boltzmann probability is calculated assuming that the interaction energy is proportional to the contact area given in Table 1.
Step 3: using information from Table 1, the number of active sites available for interaction is obtained.
Step 4: return to Step 2 until $N$ is reached.

For a given number $N$ of dimers, random sets of arrangements for the polyhedrons on the AFM tip surface were generated. The average number of active sites available for interacting with the substrates is obtained in Step 3 at the end of the iterative stochastic procedure. Note that the number of active sites is smaller than the number of adsorbed enzymes because some sites are not exposed to the substrates, as will be discussed later on.

### 2.4. Steered molecular dynamics

Steered molecular dynamics (SMD) [10,28] calculations were carried out to simulate the average force required to detach the herbicide diclofop from the ACC active site cavity. As shown in Fig. 4, a vector toward the entrance of the active site was imposed to represent the pathway for detachment of the diclofop molecule. The calculations were performed using GROMACS computational package version 4.5.4 [8,29] with the following protocol: (i) the enzyme structure reported by Franca et al. was solvated by SPC [30] water molecules and ions were added to balance/equilibrate charge distribution in the system; (ii) the calculations were performed in the $NpT$ ensemble at $p = 1$ bar and $T = 298$ K. Standard Berendsen barostat and Langevin thermostat procedures implemented in GROMACS were used; (iii) a cutoff radius of 1.4 nm was used and long range corrections for electrostatic potential were considered using the Particle Mesh Ewald (PME) formalism; (iv) using a 1 fs time step for integration, equilibrium was achieved within a 50 ps $NVT$ calculations and a further 1 ns $NpT$ trajectory was used for averaging; (v) a constant force of 3670 pN nm$^{-1}$ and a speed rate of 0.001 nm/ps were used in the detachment process.
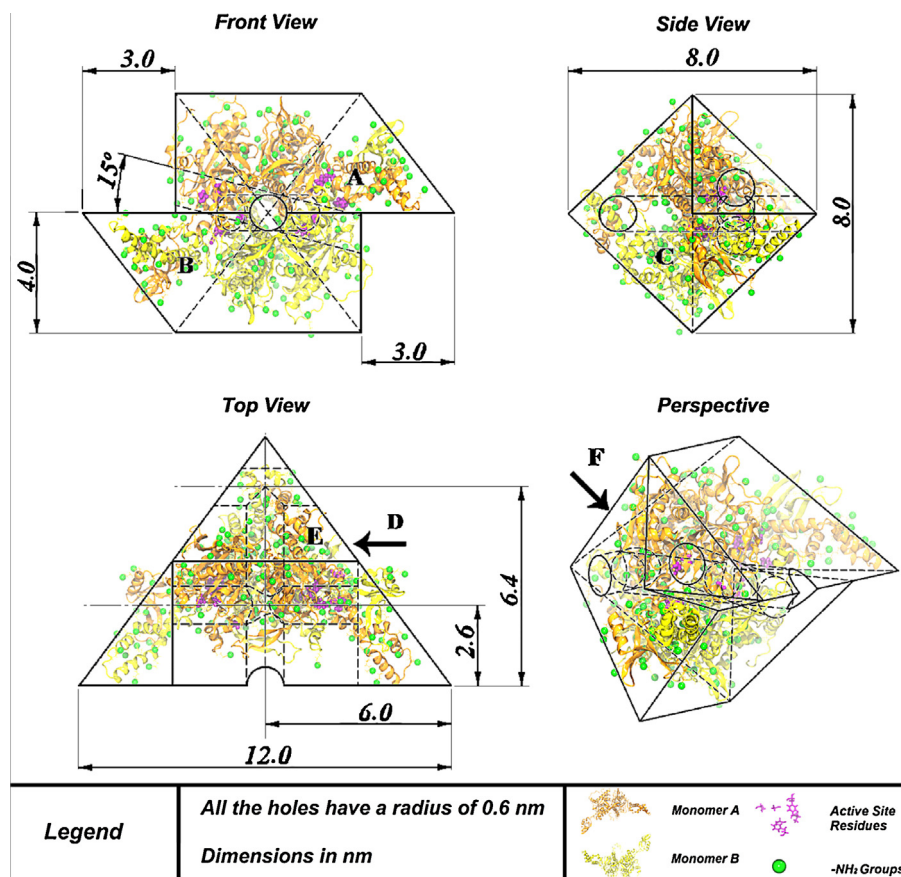
**Fig. 2.** Proposed rigid model of the ACC enzyme according to its dimensions.
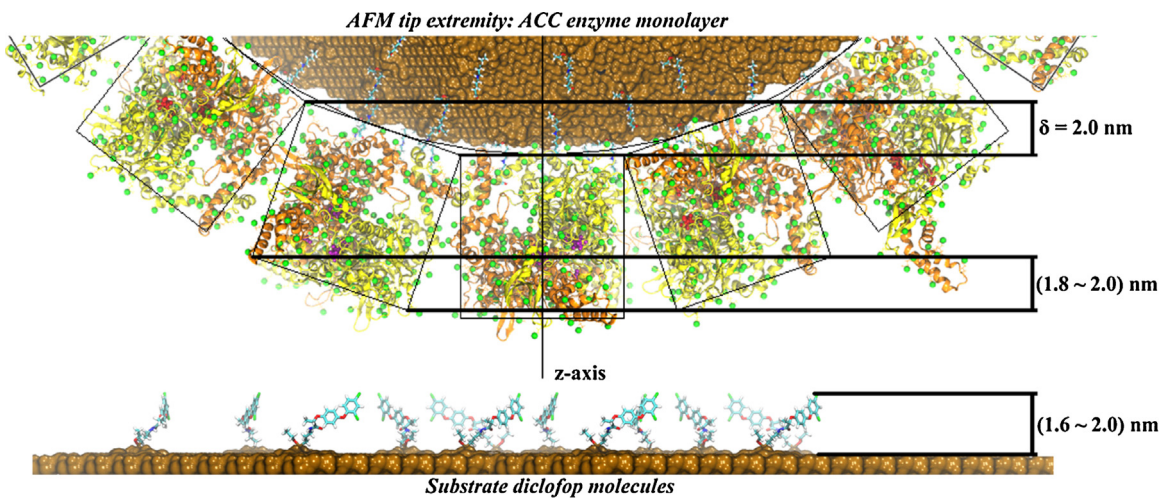


**Fig. 3.** Schematic monolayer section of both substrate surface and AFM tip radius covered by diclofop molecules and ACC enzymes respectively.
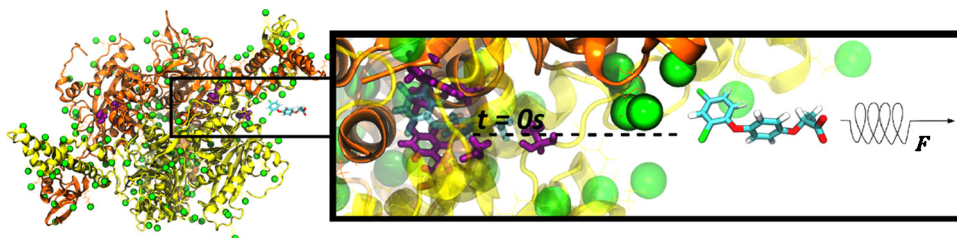


**Fig. 4.** Steered molecular dynamics representation of the herbicide diclofop decoupling process from the active site of the ACC enzyme.

**Table 2**
For a given number ($N$) of enzyme dimers covering the AFM tip, estimations were made of the area of the tip covered and the average number of active sites available for interaction, in the second and third columns, respectively. Using the force obtained from SMD simulations per enzyme dimer, the theoretical force was obtained. For full coverage of the tip, $N=6$, the predicted force agrees with the experimentally measured average force from Ref. [26]. These values are highlighted in bold in the third line. Because the experimental results led to a histogram of force values, from 3 to 8 nN, it is possible to predict how many active sites are responsible for the interaction. Here, $N$ would vary from 4 to 7, as indicated in lines from 1 to 4. Results with confidence of 95%.

| Number of enzyme ($N$) | AFM tip area covered by enzymes (nm$^2$) | Average number of active sites | Theoretical force (nN) | Experimental force (nN) |
| --- | --- | --- | --- | --- |
| 4 | 139.4 | 2.53 | $4.0 \pm 1.3$ | $3.9 \pm 1.8$ |
| 5 | 174.5 | 3.20 | $5.1 \pm 1.6$ | $4.9 \pm 1.9$ |
| **6** | **208.8** | **3.86** | **$6.2 \pm 1.9$** | **$6.1 \pm 2.0$** |
| 7 | 243.5 | 4.54 | $7.2 \pm 2.3$ | $7.0 \pm 2.2$ |
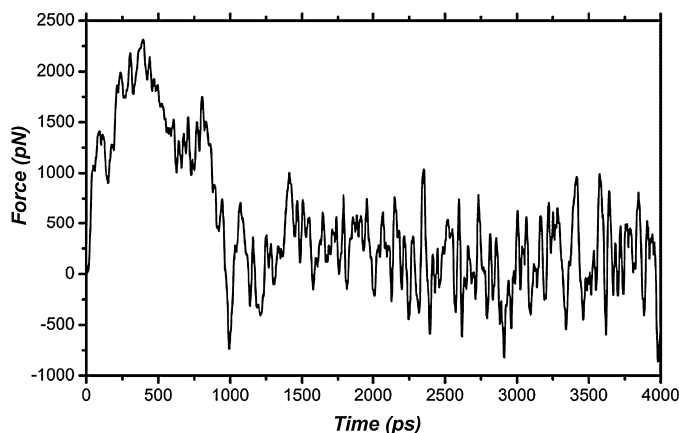


**Fig. 5.** Integrated force curve of the diclofop decoupling from the ACC active site. The calculated average force was estimated from 0 to 1500 ps time step.

## 3. Results

The force curve along the detachment pathway in Fig. 4, obtained with SMD simulations, is presented in Fig. 5. The average force was calculated in the time interval from $t=0$ to $t_f=1000$ ps, since the diclofop molecule is outside the cavity of the enzyme active site after a time $t_f$. An average force $FS=(1.6\pm0.5)$ nN was obtained per enzyme, with a confidence level of 95%. Using the technical specifications from the manufacturer, the AFM tip radius ($R$) was assumed to be $(17.5\pm2.5)$ nm. With $A=2\pi\delta R$ and $\delta=2.0$ nm, the AFM available area is $(220\pm31)$ nm$^2$.

Table 2 shows the AFM tip area covered by enzymes for a given $N$ of ACC dimers, obtained from averaging thousands of combinations of polyhedron faces generated by the stochastic program. Full coverage of the AFM tip corresponds roughly to adsorption of 6 enzyme dimers ($N=6$), to which the average number of active sites would lead to a force of $(6.2\pm1.9)$ nN, using the average force per enzyme of $(1.6\pm0.5)$ nN. The agreement with the experimental data is remarkable. For a fully covered AFM tip, Bueno et al. [26] measured forces varying from 3 to 8 nN, leading to a histogram of forces which most probable value is $(6.1\pm2.0)$ nN. These values are highlighted in line 3 of Table 2. It is also shown that the average number of active sites is smaller than $N$, as one should expect since some active sites are not exposed to the substrates and this was taken into account in our stochastic model. Moreover, with the theoretical results we may predict the number of enzymes covering the tip to account for the measured forces in the histogram, which was also indicated in Table 2.

## 4. Conclusions

In this paper we introduced a procedure that allows the estimation of the interaction force between the ACC enzyme and its substrate diclofop, as well as compare this value with experimental results from AFM experiments. This was achieved with steered molecular dynamics (SMD), where the enzyme dimers were represented as rigid polyhedrons and the coverage of the AFM tip with enzymes was simulated using a stochastic process. The dimension of each polyhedron face was calculated using routines provided by the programs [23,24,31] and the interaction energy between the enzyme and AFM tip surface was assumed to be proportional to the contact area. From geometry considerations it was possible to determine the number ($N$) of enzymes attached to the AFM tip and the average number of active sites effectively interacting with the substrate. The remarkable agreement between the theoretical and experimental results demonstrates that the procedure proposed is useful to interpret AFM experiments.

## Acknowledgements

## References

[1] V.G. Rumayor, O.R. Iglesias, L.G. Cabezas, Aplicaciones de biosensores en la industria agroalimentaria, CEIM, Mdri, 2005.
[2] D.P.E. Smith, Limits of force microscopy, Rev. Sci. Instrum. 66 (1995) 3191–3195.
[3] F.L. Leite, C.C. Bueno, A.L. Da Róz, E.C. Ziemath, O.N. Oliveira, Theoretical models for surface forces and adhesion and their measurement using atomic force microscopy, Int. J. Mol. Sci. 13 (2012) 12773–12856.
[4] A. Etchegaray, C. de, C. Bueno, O. Teschke, Identification of microcistin LR at the molecular level using atomic force microscopy, Quím. Nova 33 (2010) 1843–1848.
[5] D.K. Deda, B.B.S. Pereira, C.C. Bueno, A.N. da Silva, G.A. Ribeiro, A.M. Amarante, et al., The use of functionalized AFM tips as molecular sensors in the detection of pesticides, Mater. Res. (2013) 683–687.
[6] A. da Silva, D. Deda, A. da Róz, R. Prado, C. Carvalho, V. Viviani, et al., Nanobiosensors based on chemically modified AFM probes: a useful tool for metsulfuron-methyl detection, Sensors 13 (2013) 1477–1489.
[7] D. Van Der Spoel, GROMACS: fast, flexible, and free, J. Comput. Chem. 26 (2006) 1701–1718.
[8] S. Pronk, S. Páll, R. Schulz, P. Larsson, P. Bjelkmar, R. Apostolov, et al., GROMACS 4.5: a high-throughput and highly parallel open source molecular simulation toolkit, Bioinformatics 29 (2013) 845–854.
[9] L.V. Kalé, M. Bhandarkar, M. Bh, R. Brunner, N. Krawetz, A. Shinozaki, et al., NAMD: a Case Study in Multilingual Parallel Programming, 1997, pp. 367–381.
[10] B. Isralewitz, J. Baudry, J. Gullingsrud, D. Kosztin, K. Schulten, Steered molecular dynamics investigations of protein function, J. Mol. Graph. Model. 19 (2001) 13–25.
[11] Y.M. Rhee, V.S. Pande, Multiplexed-replica exchange molecular dynamics method for protein folding simulation, Biophys. J. 84 (2003) 775–786.
[12] A.V. Vargiu, P. Ruggerone, A. Magistrato, P. Carloni, Dissociation of minor groove binders from DNA: insights from metadynamics simulations, Nucl. Acids Res. 36 (2008) 5910–5921.
[13] H. Zhang, B. Tweel, J. Li, L. Tong, Crystal structure of the carboxyltransferase domain of acetyl-coenzyme A carboxylase in complex with CP-640186, Structure 12 (2004) 1683–1691.
[14] M.D. Devine, A. Shukla, Altered target sites as a mechanism of herbicide resistance, Crop Prot. 19 (2000) 881–889.
[15] C. Delye, X.-Q. Zhang, C. Chalopin, S. Michel, S.B. Powles, An isoleucine residue within the carboxyl-transferase domain of multidomain acetyl-coenzyme A

carboxylase is a major determinant of sensitivity to aryloxyphenoxypropionate but not to cyclohexanedione inhibitors, Plant Physiol. 132 (2003) 1716–1723.

[16] H. Zhang, Z. Yang, Y. Shen, L. Tong, Crystal structure of the carboxyltransferase domain of acetyl-coenzyme A carboxylase, Science 299 (2003) 2064–2067.

[17] Y. Sasaki, Y. Nagano, Plant acetyl-CoA carboxylase: structure, biosynthesis, regulation, and gene manipulation for plant breeding, Biosci. Biotechnol. Biochem. 68 (2004) 1175–1184.

[18] H.M. Berman, J. Westbrook, Z. Feng, G. Gilliland, T.N. Bhat, H. Weissig, et al., The protein data bank, Nucl. Acids Res. 28 (2000) 235–242.

[19] E.F. Franca, F.L. Leite, R.A. Cunha, O.N. Oliveira Jr., L.C.G. Freitas, Designing an enzyme-based nanobiosensor using molecular modeling techniques, Phys. Chem. Chem. Phys. 13 (2011) 8894–8899.

[20] G.S. Oliveira, F.L. Leite, A.M. Amarante, E.F. Franca, R.A. Cunha, J.M. Briggs, et al., Molecular modeling of enzyme attachment on AFM probes, J. Mol. Graph. Model. 45 (2013) 128–136.

[21] G.M. Morris, D.S. Goodsell, R.S. Halliday, R. Huey, W.E. Hart, R.K. Belew, et al., Automated docking using a Lamarckian genetic algorithm and an empirical binding free energy function, J. Comput. Chem. 19 (1998) 1639–1662.

[22] G.M. Morris, R. Huey, W. Lindstrom, M.F. Sanner, R.K. Belew, D.S. Goodsell, et al., AutoDock4 and AutoDockTools4: automated docking with selective receptor flexibility, J. Comput. Chem. 30 (2009) 2785–2791.

[23] A. Herráez, Biomolecules in the computer: Jmol to the rescue, Biochem. Mol. Biol. Educ. 34 (2006) 255–261.

[24] W. Humphrey, A. Dalke, K. Schulten, VMD: visual molecular dynamics, J. Mol. Graph. 14 (1996) 33–38.

[25] H. Cheng, N. Ji, Y. Peng, X. Shen, J. Xu, Z. Dong, et al., Molecular characterization and tissue-specific expression of the acetyl-CoA carboxylase α gene from Grass carp, *Ctenopharyngodon idella*, Gene 487 (2011) 46–51.

[26] C. Castro Bueno, A. Moraes Amarante, G.S. Oliveira, D. Kotra Deda, O. Teschke, E. de Faria Franca, et al., Nanobiosensor for diclofop detection based on chemically modified AFM probes, IEEE Sens. J. 14 (2014) 1467–1475.

[27] L.C.G. Freitas, Program Recover, Department of Chemistry, UFSCar, Fortran Code, 2013.

[28] S. Izrailev, S. Stepaniants, B. Isralewitz, D. Kosztin, H. Lu, F. Molnar, et al., Steered molecular dynamics, in: P. Deuflhard, J. Hermans, B. Leimkuhler, A.E. Mark, S. Reich, R.D. Skeel (Eds.), Computational Molecular Dynamics: Challenges, Methods, Ideas, Springer, Berlin/Heidelberg, 1999, pp. 39–65.

[29] B. Hess, C. Kutzner, D. van der Spoel, E. Lindahl, GROMACS 4: algorithms for highly efficient, load-balanced, and scalable molecular simulation, J. Chem. Theory Comput. 4 (2008) 435–447.

[30] H.J.C. Berendsen, J.R. Grigera, T.P. Straatsma, The missing term in effective pair potentials, J. Phys. Chem. 91 (1987) 6269–6271.

[31] F. Provenza, PRO-TEC-Desenhista de Máquinas, 46th ed., F. Provenza, 1991.